SMALL SOLIDS IN AN INVISCID FLUID

Boris Andreianov

Laboratoire de Mathématiques de Besançon
Université de Franche-Comté
25030 Besançon Cedex, France

Frédéric Lagoutière

Laboratoire de mathématiques
Université Paris-Sud
91405 Orsay cedex, France

Nicolas Seguin

UMR 7598 Laboratoire J.-L. Lions
UPMC Univ Paris 06
Paris, F-75005 France

Takéo Takahashi

Institut Élie Cartan UMR 7502
INRIA, Nancy-Université, CNRS
54506 Vandœuvre-lès-Nancy Cedex, France

Abstract. We present in this paper several results concerning a simple model of interaction between an inviscid fluid, modeled by the Burgers equation, and a particle, assumed to be point-wise. It is composed by a first-order partial differential equation which involves a singular source term and by an ordinary differential equation. The coupling is ensured through a drag force that can be linear or quadratic. Though this model can be considered as a simple one, its mathematical analysis is involved. We put forward a notion of entropy solution to our model, define a Riemann solver and make first steps towards well-posedness results. The main goal is to construct easy-to-implement and yet reliable numerical approximation methods; we design several finite volume schemes, which are analyzed and tested.

1. **Introduction.** It is well known since the works of d'Alembert that the problem of solid-fluid interaction may contain modeling issues. Indeed, he showed that a solid immersed in an inviscid fluid may not be submitted to any resultant force; in other words, birds and planes could not fly with such a model... An answer to the d'Alembert paradox has been the use of viscous models of fluid-solid interaction (see for instance the review of Hillairet [14] and [18], and references therein).

On the other hand, when the Reynolds number is great, it is reasonable to neglect the viscous effects in the model which governs the fluid. The question is thus, how to conserve any information of the vanishing viscosity? The answer,

classical in Aerodynamics for instance, is the use of the drag force. It takes the form of a source term which takes into account the difference between the velocity of the fluid and the velocity of the solid. In this paper, we restrict ourselves to the Burgers equation for the fluid in order to simplify the presentation and, basically, to have a hope to obtain fairly general mathematical results, since the analysis of compressible inviscid models is far from being completely understood. The model for the interaction, *via* a drag force, of a particle with a Burgers fluid writes

$$\partial_t u + \partial_x(u^2/2) = \lambda \, D(h'(t) - u) \, \delta_0(x - h(t)), \tag{1}$$

$$mh''(t) = \lambda \, D(u(t, h(t)) - h'(t)) \tag{2}$$

where the two unknowns are u, the velocity of the fluid, and h, the position of the solid (then h' and h'' respectively denote its velocity and its acceleration). The parameters are λ, the drag coefficient, and m, the mass of the solid; both are positive. The function D which intervenes in the drag force is an increasing odd function. Actually, we will suppose that

$$\text{either } D(v) = v \qquad\qquad \text{(the linear case)} \tag{3}$$

$$\text{or } D(v) = v|v| \qquad\qquad \text{(the quadratic case).} \tag{4}$$

Though this model seems naive, it involves several mathematical difficulties and we hope that it can reproduce some complex phenomena proper to fluid-solid inter-action. A first difficulty concerns Eq. (1): it involves the product of distributions u and δ_0, which has to be defined since u can be discontinuous at $(t, h(t))$. For the same reason, the differential equation (2) must be understood in the Carathéodory sense. Another difficulty is the numerical approximation of such a model. Since the particle is point-wise, it can be easier to locate it at each time step on an interface of the mesh. This can be done either using a moving mesh which follows the particle, or using a random sampling for choosing the new position of the particle. The latter method has the advantage to be easily extendible to the case of several particles.

Let us provide the plan of the paper. In Sec. 2, we describe the model and give the definition of solutions, based on modeling arguments. Equation (1) is understood in an entropy sense, with a particular focus on the "entropy coupling" of the states $u(t, h(t)^{\pm})$ across the trajectory $(t, h(t))$ (see Definition 2.2(i),(ii)). Equation (2) is interpreted in a precise way which means that the particle is driven by the difference of the normal fluxes of the entropy solution u of the Burgers equation at the trajectory $(t, h(t))$ (see Definition 2.2(iii)). Heading to well-posedness, we start by decoupling (2) from (1); namely, we assume that a function h is given, and we construct a unique entropy solution u to (1) in the sense of Definition 2.2(i),(ii). Sec. 3 is devoted to the analysis of Eq. (1), assuming that $h'(t)$ is a given constant. Then in Sec. 4 we treat the case of a piecewise affine h, and finally, we get well-posedness for (1) with any given trajectory $h \in C^1(\mathbb{R}^+)$. Then we sketch the existence argument for the coupled problem (1-2). In both Sec. 3 and 4 we pay a particular attention to resolution of the Riemann problems. Finally, Sec. 5 deals with the construction of solutions by finite volume schemes (first for the decoupled, and then for the coupled model (1-2)) and provides several numerical tests.

2. **Definition of solutions.** We present in this section the rigorous definition of the solutions of (1-2). To this aim, we have to provide a definition of the singular source term and of the differential equation (2).

2.1. **The non conservative product.** Before giving the details of the definition
of the non conservative product, let us rewrite the model as

$$\partial_t u + \partial_x(u^2/2) - \lambda\, D(h'(t) - u)\, \partial_x w = 0, \tag{5}$$

$$\partial_t w + h'(t)\, \partial_x w = 0, \tag{6}$$

$$mh''(t) = \lambda\, D(u(t, h(t)) - h'(t)) \tag{7}$$

with $w(0, x) = H(x)$, H being the Heaviside function (we have set $h(0) = 0$). Of
course, the models (1-2) and (5-7) are equivalent. Let us assume for a while that the
trajectory h of the particle is given and focus on the first-order system (5-6). For
each definition of the drag force, one can easily check that system (5-6) is strictly
hyperbolic when u and h' (the eigenvalues of the system) are different; further, if
$u = h'$, the dimension of the corresponding eigenspace is 2, i.e. this system is not
resonant (and thus is hyperbolic).

In order to understand the behavior of u near the particle $x = h(t)$, we enlarge
the particle replacing the initial condition for w by $w(0, x) = H_\varepsilon(x)$ where H_ε is
a smooth non decreasing function such that $H_\varepsilon(x) = H(x)$ for all $|x| > \varepsilon$. Eq.(6)
leads to the formula $w(t, x) = H_\varepsilon(x - h(t))$. We seek for solutions "inside" the
particle, of the form $U(x - h(t)) = u(t, x)$ for $|x - h(t)| \le \varepsilon$. Such solutions must
satisfy for all $t > 0$

$$(U^2/2 - h'(t)U)'(\xi) - \lambda D(h'(t) - U(\xi))H_\varepsilon'(\xi) = 0, \quad |\xi| < \varepsilon, \tag{8}$$

in the weak entropy sense. Namely, if U is discontinuous at $\xi = \xi_0$, then $(U(\xi_0^-) + U(\xi_0^+))/2 = h'(t)$ and $U(\xi_0^-) > U(\xi_0^+)$. Therefore, we claim that a pair $(u^-, u^+) \in \mathbb{R}^2$ can represent the values (more exactly, the traces) of u at $x = h(t)^\pm$ in (1-2) if
and only if there exists a weak entropy solution U to (8) such that $U(-\varepsilon) = u^-$ and
$U(\varepsilon) = u^+$. In the spirit of [1] and [2], we call the set of such couples *admissibility
germ* (germ, for short). After a careful study (see [18] for the case of a linear drag
force (3)), we are able to describe the admissibility germ corresponding to a particle
of velocity $h'(t)$:

Proposition 2.1. *(i) If the drag force is linear (i.e. D is defined by (3)), then the
admissibility germ is*

$$\mathcal{G}_l(h'(t)) = (h'(t), h'(t)) + \{(c_-, c_+) \in \mathbb{R}^2 \mid c_- - c_+ = \lambda\}$$
$$\cup \{(c_-, c_+) \in \mathbb{R}_+ \times \mathbb{R}_- \mid -\lambda \le c_- + c_+ \le \lambda\}. \tag{9}$$

*(ii) If the drag force is quadratic (i.e. D is defined by (4)), then the admissibility
germ is*

$$\mathcal{G}_q(h'(t)) = (h'(t), h'(t)) + \{(c_-, c_+) \in \mathbb{R}^2 \mid c_+ = c_- e^{-\operatorname{sgn}(c_-)\lambda}\}$$
$$\cup \{(c_-, c_+) \in \mathbb{R}_+ \times \mathbb{R}_- \mid -e^\lambda \le c_+/c_- \le -e^{-\lambda}\}. \tag{10}$$

It is worth noting that the germs $\mathcal{G}_l$ and $\mathcal{G}_q$ are independent of ε and of the
regularization H_ε, but they depend on λ and $h'(t)$ (see Fig. 1). Because we fix λ,
we do not stress the dependence of $\mathcal{G}_{l,q}(h'(t))$ on λ.

At this stage, assuming $h \in \mathcal{C}^1(\mathbb{R}_+)$, one could define an admissible solution u
of (1) with drag force (3) (resp., (4)) as a classical Kruzhkov solution for $x \ne h(t)$,
whose couple of traces $(u(t, h(t)^-), u(t, h(t)^+))$ at $x = h(t)^\pm$ belongs to the germ $\mathcal{G}_l$
(resp., to the germ $\mathcal{G}_q$). Here and in the sequel,

$$u \in L^\infty(\mathbb{R}_+ \times \mathbb{R}) \;\mapsto u(\cdot, h(\cdot)^-) \in L^1_{loc}(\mathbb{R}_+)$$
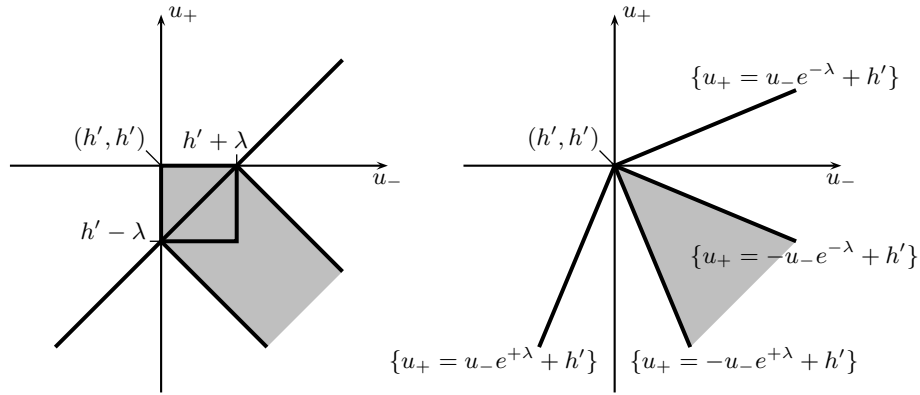
FIGURE 1. Representation of the germs $\mathcal{G}_l$ (left) and $\mathcal{G}_q$ (right).

is the strong L^1_{loc} trace operator in the sense of Panov [19] on the C^1 curve $\{x = h(t)\}$ from the left (and the trace operator on the curve $\{x = h(t)\}$ from the right is defined analogously). Because u is a classical Kruzhkov solution for $x \neq h(t)$, the strong traces $u(t, h(t)^{\pm})$ do exist, according to [19].

2.2. **The differential equation.** It remains to give a precise definition for the ordinary differential equation (2). First, let us note that the source term in (1) is exactly the opposite of the right-hand side of (2). This formally provides the conservation of the total impulsion:

$$\frac{d}{dt}\left(\int_{\mathbb{R}} u \, dx + mh'\right) = 0. \tag{11}$$

Note that this equation is also valid in the weak sense. As a result, this property of conservation can replace the ODE (2) and one can derive a precise definition for (2) by a local balance in the neighborhood of the particle (in the same spirit as the derivation of the Rankine-Hugoniot jump relations for conservation laws):

Proposition 2.2. *If the solution of (1-2) complies with the conservation of the total impulsion (11), then the ODE (2) can be written*

$$\begin{aligned}
mh''(t) &= \left(u(t, h(t)^-)^2/2 - h'(t)u(t, h(t)^-)\right) \\
&\quad - \left(u(t, h(t)^+)^2/2 - h'(t)u(t, h(t)^+)\right),
\end{aligned} \tag{12}$$

whatever the drag force is.

Remark that D and λ appear implicitly in (12) since all the informations related to the source term have already been enclosed in the admissible germs.

Furthermore, notice that the right-hand side of (12) is expressed as the difference of the normal components of the 2D-field $(u, u^2/2)$ on the curve $\{x = h(t)\}$ from the left and from the right. Combining this observation with the Green-Gauss formula, we get the following weak formulation of (2):

Lemma 2.1. *Let $h \in W^{2,\infty}(0, T)$; let u be an entropy solution of (1) on $\{x \neq h(t)\}$. Then $h(\cdot)$ verifies (12) if and only if for all $\xi \in \mathcal{D}([0, T))$, for all $\psi \in \mathcal{D}(\mathbb{R})$ such*

that $\psi \equiv 1$ on the set $\{x \in \mathbb{R} : \exists t \in [0,T] \text{ such that } h(t) = x\}$, there holds

$$-m \int_0^T h'(t)\xi'(t)dt = mh'(0)\xi(0) + \int_0^T \int_{\mathbb{R}} \left[u\psi\xi'(t) + \frac{u^2}{2}\xi\psi'(x) \right] + \int_{\mathbb{R}} u_0\psi\xi(0).$$

From the above formula we also see that the existence of strong traces $u(t, h(t)^{\pm})$ is not necessary in order to give sense to the ODE (12).

2.3. **The full model.** We are now in position to give a rigorous definition of solution for the Cauchy problem, i.e. system (1-2) with the initial conditions

$$u(0,x) = u_0(x) \quad \forall x \in \mathbb{R}, \tag{13}$$

$$(h(0), h'(0)) = (h_0, v_0). \tag{14}$$

Definition 2.2. Assume that $u_0 \in L^\infty(\mathbb{R})$ and $v_0 \in \mathbb{R}$. A pair $(u, h) \in L^\infty(\mathbb{R}_+ \times \mathbb{R}) \times \mathcal{C}^1(\mathbb{R}_+)$ is an *entropy solution* of the Cauchy problem (1-2)-(13-14) with the drag force (3) (respectively (4)) if

    i. u is a Kruzhkov entropy solution for the Burgers equation with initial datum (13) on the domain $\{x < h(t), t \geq 0\} \cup \{x > h(t), t \geq 0\}$;

    ii. the couples of one-sided traces of u on $\{x = h(t)\}$ are in the germ:

    for a.e. $t > 0$, $\quad (u(t, h(t)^-), u(t, h(t)^+)) \in \mathcal{G}_l(h'(t))$ (resp. $\in \mathcal{G}_q(h'(t))$);

    iii. h satisfies the ordinary differential equation (12) with initial data (14).

As pointed out hereabove, the point i. of the definition guarantees the existence of traces of u used in the points ii.,iii. of the definition. Yet the explicit use of traces in Definition 2.2 may be a disadvantage, for instance when the stability of solutions or convergence of approximate solutions is studied. Therefore we will also use equivalent formulations, including the formulation of Lem. 2.1 (instead of Def. 2.2 iii.) for the ODE (2), and the global "adapted entropies" formulation of Prop. 3.1 below (instead of Def. 2.2 i.,ii.) for the PDE (1).

Now let us give the reasons for which we believe that the above formulation is "the good one" for the problem considered. First, as a preliminary step to a resolution of (1-2) we will also consider Eq. (1) in the entropy sense of Def. 2.2 i.,ii. with a given particle trajectory $h \in C^1(\mathbb{R}_+)$. For this case, we readily get the uniqueness, L^1 contraction and comparison result:

Theorem 2.3. *Assume that a trajectory $h \in C^1(\mathbb{R}_+)$ is given. Let u (resp. $\hat{u}$) be an entropy solution of (1) in the sense of Def. 2.2 i.,ii. with the initial datum u_0 (resp., with the initial datum $\hat{u}_0$). Then for a.e. $t > 0$,*

$$\int (u - \hat{u})^+(t) \leq \int (u_0 - \hat{u}_0)^+. \tag{15}$$

The proof (cf. [1, 2]) is straightforward from the Kato inequality for entropy solutions in the domain $\{x \neq h(t)\}$, from the definition of strong traces on the curve $\{x = h(t)\}$ and from the key dissipation property of the germs $\mathcal{G}_l, \mathcal{G}_q$:

Lemma 2.4. *Set $\Phi(a, b) = \text{sgn}(a-b)(\frac{a^2}{2} - \frac{b^2}{2})$. For all $(c_L, c_R) \in \mathcal{G}$ and $(d_L, d_R) \in \mathcal{G}$ (where $\mathcal{G} = \mathcal{G}_l(h'(t))$ or $\mathcal{G}_q(h'(t))$ according to the drag force), we have*

$$\left(\Phi(c_R, d_R) - h'(t)|c_R - d_R| \right) - \left(\Phi(c_L, d_L) - h'(t)|c_L - d_L| \right) \leq 0.$$

The lemma is justified by a case study (see [3]).

In addition to the above uniqueness claim, existence of the solutions studied in Thm. 2.3 will be justified in Thm. 4.2 below. The main ingredient of the existence proof is the convergence analysis of the numerical scheme given in Sec. 5.1. An important point is the following L^∞ bound:

Lemma 2.5. *For each of the cases (3), (4), there exists a constant $C = C(\|u_0\|_\infty, \lambda)$ such that $\|u\|_\infty \leq C$, where u is an entropy solution of (1)-(13) with some given function $h \in C^1(\mathbb{R})$.*

Finally, note the following result whose proof is rather technical (see [4]):

Theorem 2.6. *Assume that the initial data u_0, h_0 and v_0 are fixed. Consider $E := \{h \in C^1(\mathbb{R}) : h(0) = h_0, h'(0) = v_0\}$ endowed with the $C^1(\mathbb{R})$ topology, and $F := L^\infty(\mathbb{R}_+ \times \mathbb{R})$ endowed with the L^1_{loc} topology. Then the unique entropy solution $u \in F$ of (1)-(13) depends continuously on $h \in E$.*

Thus not only the problem (1)-(13) in the sense of Def. 2.2 i.,ii. is well-posed for $h(\cdot)$ given, but also the solution depends on h continuously. Hence we will deduce an existence result for the coupled problem (1-2)-(13-14) with the help of a fixed-point argument developed in Sec. 4.

The two following sections contain an account on our results on construction of solutions. As it is usual in the context of hyperbolic conservation law, we pay a particular attention to the resolution of the Riemann problem.

3. **Construction of solutions: The case of a particle with a constant velocity.** We are interested now in an efficient construction of solutions of the Riemann and the Cauchy problem for (1-2). First, we focus on the resolution of equation (1) (in the sense of Def. 2.2 i.,ii.) for the case of a particle having a zero velocity (the extension to the case of a constant velocity V is straightforward, setting $\tilde{u} = u - V$ and $\tilde{x} = x - Vt$). The model writes

$$\partial_t u + \partial_x(u^2/2) + \lambda \, D(u) \, \delta_0 = 0. \tag{16}$$

As mentioned above, this equation is not resonant and thus, it does not enter in the frame studied Isaacson and Temple [15]. Nonetheless, its well-posedness cannot be directly concluded, due to the singular term $D(u) \, \delta_0$ (see Remark 1).

3.1. **The Riemann problem.** We first study the Riemann problem, that is to say Eq. (16) with the initial condition

$$u(0, x) = \begin{cases} u_L & \text{if } x < 0, \\ u_R & \text{if } x > 0, \end{cases} \tag{17}$$

where $u_L, u_R \in \mathbb{R}$. In order to solve (16-17), we introduce the sets $\mathcal{U}_-(u_0)$ and $\mathcal{U}_+(u_0)$ which are respectively the sets of states which can be connected to u_0 by waves with non-positive and nonnegative speeds. Classical computations give

$$\mathcal{U}_-(u_0) = (-\infty, 0\bot(-u_0)] \cup \{u_0\} \quad \text{and} \quad \mathcal{U}_+(u_0) = [0\top(-u_0), +\infty) \cup \{u_0\},$$

where $a\top b = \max(a, b)$ and $a\bot b = \min(a, b)$. As a result, the solution to the Riemann problem reduces to find two states u_- and u_+ such that

- $u_- \in \mathcal{U}_-(u_L)$,
- $u_+ \in \mathcal{U}_+(u_R)$,
- $(u_-, u_+) \in \mathcal{G}$ (where $\mathcal{G} = \mathcal{G}_l$ or $\mathcal{G}_q$ according to the drag force).

It has been resolved in [18] in the case of the linear drag force and a similar reasoning can be performed for the quadratic drag force:

Theorem 3.1. *If D is defined by (3) or (4), the Riemann problem (16-17) admits one and only one self-similar solution.*

We do not prove this theorem (for D given by (3), see the *proof* in [18]) but only provide the partition of the (u_L, u_R)-plane and the associated configurations of waves (see Fig. 2).
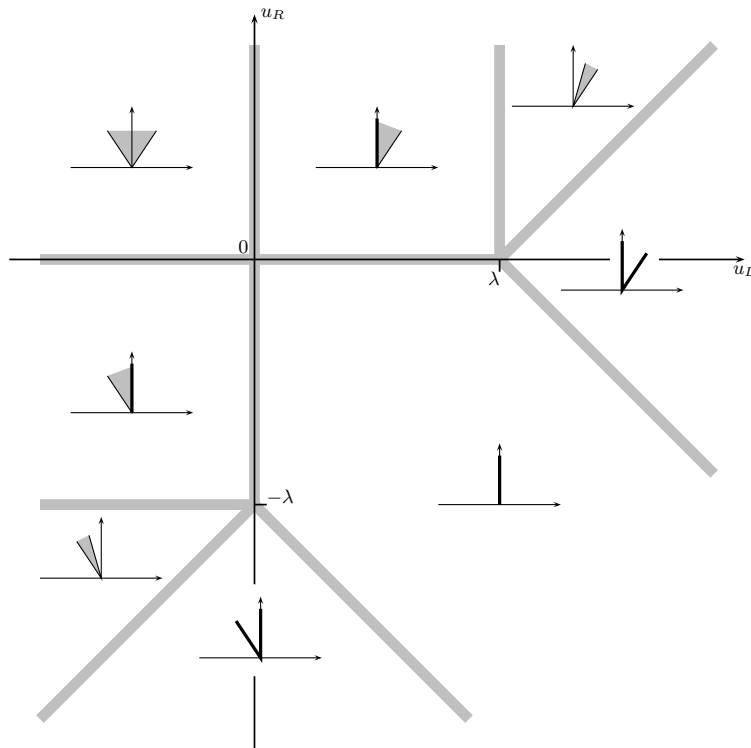

FIGURE 2. Configurations of waves for the case of a linear drag force (3) with $h'(t) = 0$.

Remark 1. Surprisingly, uniqueness does not hold true when focusing on the linear drag force but with $\lambda < 0$. Consider the equation $\partial_t u + \partial_x(u^2/2) - u\,\delta_0 = 0$ and the initial condition $u(0, x) = 0$ for all $x \in \mathbb{R}$. Of course $u(t, x) = 0$ for all $(t, x) \in \mathbb{R}_+ \times \mathbb{R}$ is solution, but also

$$u(t, x) = \begin{cases} 0 & \text{if } |x/t| > \alpha/2, \\ -\alpha & \text{if } -\alpha/2 < x/t < 0, \\ \alpha & \text{if } 0 < x/t < \alpha/2, \end{cases}$$

for any $0 < \alpha \leq 1/2$. On the other hand, let us recall that in the resonant case studied by Isaacson and Temple [15], up to three (self-similar) solutions may coexist.
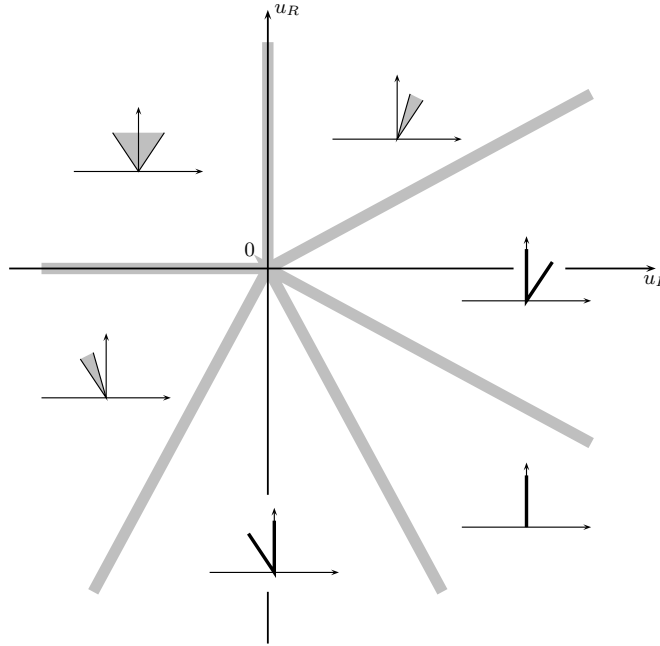
FIGURE 3. Configurations of waves for the case of a quadratic drag force (4) with $h'(t) = 0$.

3.2. **The Cauchy problem.** Let us now focus on the Cauchy problem (16)-(13). All the details and proofs can be found in a forthcoming paper [3]. Recall that the entropy solution for this problem is a function $u \in L^\infty(\mathbb{R}_+ \times \mathbb{R})$ that fulfills Def. 2.2 i.,ii. Using the so-called *adapted Kruzhkov entropies* (see [8, 6, 10, 1, 2]), an alternative characterization of entropy solution can be given:

Proposition 3.1. *A function $u \in L^\infty(\mathbb{R}_+ \times \mathbb{R})$ is an entropy solution for (16) if and only if it satisfies, for all $(c_L, c_R) \in \mathcal{G}$ (where $\mathcal{G} = \mathcal{G}_l(0)$ or $\mathcal{G}_q(0)$ according to the drag force),*

$$\partial_t |u - c| + \partial_x \Phi(u, c) \le 0 \quad in \ \mathcal{D}'(\mathbb{R}^+ \times \mathbb{R}), \tag{18}$$

where $c(x) = c_L + (c_R - c_L)\mathbf{1}_{\mathbb{R}_+}(x)$ and $\Phi(a, b) = \text{sgn}(a - b)(a^2/2 - b^2/2)$.

From Def. 2.2 ii. (or from (18) and Lem. 2.4), it is clear that the stationary weak solutions of (16) under the form $c(x) = c_L + (c_R - c_L)\mathbf{1}_{\mathbb{R}_+}(x)$, $(c_L, c_R) \in \mathcal{G}_{l,q}(0)$, are entropy solutions. Thus formulation (18) states a localized contraction property (known as the Kato inequality) with respect to these "reference solutions". Thus formulation (18) has the same meaning as the original Kruzhkov definition, which is valid only for the case where constants are the admissible "reference solutions".

It should be stressed that the characterization (18) implies the classical Kruzhkov formulation for $\{x < 0\}$ (respectively for $\{x > 0\}$), since for any $c_L \in \mathbb{R}$ (resp. $c_R \in \mathbb{R}$) there exists at least one pair $c = (c_L, c_R) \in \mathcal{G}$. Let us also point out that one can write entropy inequalities of the kind (18) for all couples $(c_L, c_R) \in \mathbb{R}^2$, at the price of incorporating an error term $Const(\|u_0\|_\infty, \lambda) \, \text{dist}\Big((c_L, c_R), \mathcal{G}\Big)\delta_0$, $\mathcal{G} = \mathcal{G}_l(0)$ or $\mathcal{G} = \mathcal{G}_q(0)$, at the right-hand side of (18). This is necessary in order to give an analogous formulation for the case of nonconstant h', i.e. for the case

where $\mathcal{G} = \mathcal{G}_{l,q}(h'(t))$ (*cf* [17] where global entropy inequalities are used in the context of a conservation law with flux discontinuous along time-space curves; see also [22, 16, 20, 7]). We refer to [1] and to cite [3] for technical details.

The existence for the adapted entropy formulation (18) is a byproduct of the construction of Sec. 5, where a well-balanced numerical scheme is presented and its convergence is justified; here "well-balanced" means that the scheme preserves a sufficiently large family of the stationary solutions $c(x) = c_L + (c_R - c_L)\mathbf{1}_{\mathbb{R}_+}(x)$, which greatly facilitates the passage to the limit in the discrete analogue of (18).

4. **Construction of solutions: The full model.** We now focus on the full model (1-2). A tricky analysis can provide the following result:

Theorem 4.1. *For any $\lambda, m > 0$ and $u_L, u_R, v_0 \in \mathbb{R}$, the Riemann problem (1-2)-(17)-(14) admits at least one solution, in the sense of Def. 2.2, with D given by (3).*

The existence of a solution is proved by construction in [18] and uniqueness is still an open question. Moreover, the case of a quadratic drag force (4) has not been studied. Note that the asymptotic behavior of the solution constructed in [18] (as $t \to +\infty$ or as $\lambda \to +\infty$) has been investigated: the solution u converges to a solution of the classical Burgers equation and $h'(t)$ tends to a predictable constant.

We now turn to the issue of existence of a solution to the Cauchy problem. There is no true construction (yet we believe that the numerical methods of Sec. 5 may provide one), but a fixed-point technique is applied. Indeed, we first exploit the existence of solution to the case of a particle with constant velocity in order to construct a solution to (1)-(13) with a piecewise constant $h'(\cdot)$. The argument here is a simple partition of the time interval into smaller time intervals with constant h'. Then we fix $h \in C^1(\mathbb{R})$ and approximate it by piecewise affine continuous functions h_m. The sequence of the corresponding entropy solutions $(u_m)_m$ of (1) is bounded in $L^\infty(\mathbb{R}_+ \times \mathbb{R})$ by a constant that only depends on λ and $\|u_0\|_\infty$. By the standard strong precompactness results for entropy solutions of the Burgers equation, which must be combined with a diagonal extraction argument in order to cover every neighbourhood of $\{x = h(t)\}$, we can extract an a.e. convergent subsequence whose limit is denoted by u. Then we pass to the limit in the adapted entropy formulation of the kind (18), using the fact that $\text{dist}\left(\mathcal{G}_{l,q}(h'_m(t)), \mathcal{G}_{l,q}(h'(t))\right)$ goes to zero for a.e. $t > 0$, as $m \to \infty$. We conclude that u is a solution to (1)-(13). Thus, combining Thm. 2.3 with the existence result obtained, we get

Theorem 4.2. *For all given $h \in C^1(\mathbb{R}_+)$, for all $u_0 \in L^\infty(\mathbb{R})$ there exists a unique entropy solution of (1) in the sense of Def. 2.2 i.,ii. with the initial datum u_0.*

The final step is to fix u_0, h_0, v_0, to fix $T > 0$ and to define
$$S := \{h \in C^1[0,T] \; : \; h(0) = h_0, h'(0) = v_0\} \text{ endowed with the } C^1[0,T] \text{ norm.}$$
We also set $R := L^\infty((0,T) \times \mathbb{R})$ endowed with the norm $\int_0^T \int_{\mathbb{R}} |u(t,x)|e^{-|x|} \, dxdt$. Then the map $\mathcal{A}$ is defined as the composition $\mathcal{B} \circ \mathcal{C}$, where
$$\mathcal{C} : \; h \in S \; \mapsto \; (h,u) \in S \times R, \;\; u \text{ is the entropy solution given by Thm. 4.2;}$$
$$\mathcal{B} : \; (h,u) \in S \times R \; \mapsto \; \tilde{h} \in S, \;\; m\tilde{h}''(t) \text{ being given by the right-hand side of (12).}$$
It is easy to see that the image of $\mathcal{A}$ is bounded in $W^{2,\infty}(0,T)$, thus it is compact in E. The continuity of $\mathcal{C}$ is stated in Thm. 2.6. The continuity of $\mathcal{B}$ follows from

the idea of Lem. 2.1; more specifically, we are able to justify that $\tilde{h}''_m \to \tilde{h}''$ weakly in $L^1(0,T)$, whenever $h_m \to h$ in E and $u_m \to u$ in $L^1_{loc}((0,T) \times \mathbb{R})$. Thus $\mathcal{A}$ is continuous and its image is compact; restricting $\mathcal{A}$ to a large ball, we can apply the Schauder fixed-point theorem and eventually get

Theorem 4.3. *For all given $u_0 \in L^\infty(\mathbb{R})$, for all $h_0, v_0 \in \mathbb{R}$ there exists at least one entropy solution of (1-2)-(13-14) in the sense of Def. 2.2.*

5. **Numerical methods.** The numerical approximation of (1-2) is not easy and several strategies can be proposed. As in the analysis of the model, we split our study in two cases: the case where the particle has a given constant velocity and the full model. Note that we add ourselves another constraint: the numerical method must be as simple as possible in order to be extendible to more complex models, up to the multidimensional Euler equations for the fluid with several point-wise particles. Therefore, we will try to avoid as much as possible the tracking of the particle (using remeshing) and complex Riemann solvers. In the following, we provide several progresses toward this challenging goal.

5.1. **The case of a particle with a constant velocity.** In order to have an accurate account of the influence of the particle, it would be convenient to locate it at an interface of the mesh at each time step. But, if v_0 denotes the constant velocity of the particle, the case $v_0 \neq 0$ is very different from the case $v_0 = 0$. Indeed, in the latter case, the particle is always placed at the same interface while if $v_0 \neq 0$, an additional treatment must be performed for the displacement of the particle — modification of the mesh or relocating by a random sampling — since the CFL condition implies in general $v_0 \Delta t < \Delta x$. Moreover, we want to avoid the use of the exact Riemann solver for the model with interaction.

Let us focus on the simplest case: $v_0 = 0$ (see [3] for the details). Assume that $x_{i+1/2} = i\Delta x$ where Δx is the space step and note $K_i = [x_{i-1/2}, x_{i+1/2}[$, denote by Δt the time step and by u_i^n, an approximation of u at time $n\Delta t$ in K_i. Away from $x_{1/2}$, the numerical scheme is classical:

$$u_i^{n+1} = u_i^n - \frac{\Delta t}{\Delta x}(g(u_i^n, u_{i+1}^n) - g(u_{i-1}^n, u_i^n)) \quad \forall i \neq 0, 1, \tag{19}$$

and near the "particle", the scheme writes

$$u_0^{n+1} = u_0^n - \frac{\Delta t}{\Delta x}(g^-(u_0^n, u_1^n) - g(u_{-1}^n, u_0^n)),$$
$$u_1^{n+1} = u_1^n - \frac{\Delta t}{\Delta x}(g(u_1^n, u_2^n) - g^+(u_0^n, u_1^n)). \tag{20}$$

Here the numerical flux g is assumed to be monotone and consistent with the flux of the Burgers equation, while the numerical fluxes g^- and g^+ must account for the singular source term. A direct approach is to use the exact Riemann solver of Thm. 3.1 and take the states at $x/t = 0^\pm$ in order to construct the numerical flux $g^\pm$. Here we pursue another approach. We use well-balance schemes in the spirit of LeRoux and co-workers [13, 12], which are much easier to implement than the exact Riemann solver. Let us introduce the following notation (cf. Fig. 1):

$$\phi_l^-(s) = s + \lambda, \qquad \phi_l^+(s) = s - \lambda,$$
$$\phi_q^-(s) = s\, e^{\mathrm{sgn}(s)\lambda}, \quad \phi_q^+(s) = s\, e^{-\mathrm{sgn}(s)\lambda}. \tag{21}$$

These functions are needed to define the following subsets of $\mathcal{G}_{l,q}$:

$$\mathcal{G}_{l,q}^0 := \{(u^-, \phi_{l,q}^+(u^-)), u^- \in \mathbb{R}\} = \{(\phi_{l,q}^-(u^+), u^+), u^+ \in \mathbb{R}\} \quad \subset \quad \mathcal{G}_{l,q}.$$

In a sense, our numerical method will act "as if" $\mathcal{G}_{l,q}$ were simply reduced to $\mathcal{G}_{l,q}^0$. Namely, we define the numerical flux at the interface by

$$g^-(a,b) = g(a, \phi_\alpha^-(b)) \quad \text{and} \quad g^+(a,b) = g(\phi_\alpha^+(a), b), \quad \alpha = l, q. \tag{22}$$

By the consistency of g and the definition (22), this scheme verifies the *well-balance property* for solutions of (16) of the form $u(t,x) = c_L + (c_R - c_L)\mathbf{1}_{\mathbb{R}_+}$, $(c_L, c_R) \in \mathcal{G}_{l,q}^0$:

Proposition 5.1. *Consider the initial datum $u_i^0 = c_L + (c_R - c_L)\mathbf{1}_{\{i>0\}}$ with $(c_L, c_R) \in \mathcal{G}_{l,q}^0$. Then, the numerical scheme (19-22) exactly preserves this initial profile, i.e.*

$$u_i^n = c_L + (c_R - c_L)\mathbf{1}_{\{i>0\}}, \quad \forall n \geq 0.$$

Of course, this property for the numerical scheme (19-22) does not hold true in general if $\mathcal{G}_{l,q}^0$ is replaced by $\mathcal{G}_{l,q}$. But, for the case of a quadratic drag force (4), it turns out that $\mathcal{G}_q^0$ is a "sufficiently large" part of $\mathcal{G}_q$, in the sense that one can restrict (18) to couples $(c_L, c_R) \in \mathcal{G}_q^0$ and get *the same* notion of solution (see Lem. 5.2 ii. below; cf. the notion of an (A, B)-connection in [5, 10] and the notion of a definite germ in [1, 2]). For the case of a linear drag force (3), the restriction of inequalities (18) to couples $(c_L, c_R) \in \mathcal{G}_l^0$ would weaken the notion of solution (so that uniqueness would be lost); fortunately, we have the following convergence result, to be combined with Lem. 5.2 i.:

Lemma 5.1. *Let us consider the case of the linear drag force (3) and an initial datum $u_i^0 = c_L + (c_R - c_L)\mathbf{1}_{\{i>0\}}$ with $(c_L, c_R) \in [0, \lambda] \times [-\lambda, 0]$. Then, under a classical CFL condition, the numerical scheme (19-22) converges in $L_{loc}^1((\mathbb{R}^+ \times \mathbb{R})$ and a.e. to the solution $u(t,x) = c_L + (c_R - c_L)\mathbf{1}_{\mathbb{R}_+}$ of (16) as $\Delta x \to 0$.*

Let us sketch the proof. Let us look at the first time step. Since $c_R \in [-\lambda, 0]$, we have $\phi_l^-(c_R) = c_R + \lambda \in [0, \lambda]$. Therefore, the restriction to $\{i \leq 0\}$ of the numerical scheme (19-22) corresponds to a classical numerical approximation of an initial boundary-value problem for $x \in \mathbb{R}_-$ with some Dirichlet boundary datum in $[0, \lambda]$ and the initial datum $c_L \in [0, \lambda]$. Therefore for $n = 1$, we get $0 \leq u_i^n \leq \lambda$, $i \leq 0$. The same reasoning can be done for $\{i > 0\}$; we conclude that for $n = 1$, $-\lambda \leq u_i^n \leq 0$, $i > 0$. By induction, the above inequalities are extended to all $n > 0$. Thus our scheme is precisely a classical monotone consistent finite volume scheme for the Cauchy-Dirichlet problem in $\mathbb{R}_+ \times \mathbb{R}_-$; the Dirichlet datum for u_i^n, $i \leq 0$, $n > 0$ is nonnegative at each time step, and the initial datum c_L is a nonnegative constant. In such configuration, it is well known that the numerical scheme converges to c_L, since the boundary condition at $\{x = 0\}$ is inactive. The same convergence argument applies on $\mathbb{R}_+ \times \mathbb{R}_+$, the limit being the constant c_R.

In order to justify the convergence of the scheme, we need to compare two sequences given by the same numerical scheme (19-22), but with different data:

Proposition 5.2. *Consider two initial data $u_0, v_0 \in L^\infty(\mathbb{R})$ and the two corresponding sequences $(u_i^n)_{i,n}$ and $(v_i^n)_{i,n}$ given by the numerical scheme (19-22). Then, under a classical CFL condition, we have for all $n \geq 0$ and $i \in \mathbb{R}$*

$$\frac{|u_i^{n+1} - v_i^{n+1}| - |u_i^n - v_i^n|}{\Delta t} + \frac{G_{i+1/2}^{n-} - G_{i-1/2}^{n+}}{\Delta x} \leq 0, \tag{23}$$

$$G_{i+1/2}^{n\pm} = g(u_i^n \top v_i^n, u_{i+1}^n \top v_{i+1}^n) - g(u_i^n \bot v_i^n, u_{i+1}^n \bot v_{i+1}^n) \quad if\ i \neq 0,$$
$$and \quad G_{1/2}^{n\pm} = g^{\pm}(u_0^n \top v_0^n, u_1^n \top v_1^n) - g^{\pm}(u_0^n \bot v_0^n, u_1^n \bot v_1^n).$$

This result follows from the monotonicity of the numerical scheme, i.e. from the fact that, under the CFL condition, u_i^{n+1} is a non decreasing function of u_{i-1}^n, u_i^n and u_{i+1}^n, and that the functions $\phi_\alpha^{\pm}$ are increasing. Hence by a simple summation-by-parts argument, we readily deduce the discrete Kato inequality:

Proposition 5.3. *Let* $(u_i^n)_{i,n}$ *and* $(v_i^n)_{i,n}$ *be as in Prop.* 5.2. *Let* $\varphi \in \mathcal{D}([0,T) \times \mathbb{R})$, $\varphi \geq 0$, *and* $\varphi_i^n = \varphi(n\Delta t, i\Delta x)$. *Then*

$$\Delta t \Delta x \sum_{i \in \mathbb{Z}, n \in \mathbb{N}} |u_i^{n+1} - v_i^{n+1}| \frac{\varphi_i^{n+1} - \varphi_i^n}{\Delta t} + \Delta x \sum_{i \in \mathbb{Z}} |u_i^0 - v_i^0| \varphi_i^0$$

$$+ \Delta t \Delta x \sum_{i \in \mathbb{Z}^*, n \in \mathbb{N}} G_{i+1/2}^{n\pm} \frac{\varphi_{i+1}^{n+1} - \varphi_i^{n+1}}{\Delta x} + \Delta t \sum_{n \in \mathbb{N}} \varphi_0^n \left(G_{1/2}^{n-} - G_{1/2}^{n+} \right) \geq R(\varphi), \quad (24)$$

where $R(\varphi)$ *is a remainder term which vanishes as* $\Delta t, \Delta x$ *go to zero. Moreover,* $R(\varphi)$ *is zero whenever* $\varphi(t, \cdot)$ *is constant, for a.e.* t.

To continue, we need an additional assumption on the numerical flux g (we only provide a sufficient, but more readable condition):

$$\partial_a(\partial_a g(a,b) + \partial_b g(a,b)) \geq 0 \quad and \quad \partial_b(\partial_a g(a,b) + \partial_b g(a,b)) \geq 0. \quad (25)$$

Actually, classical numerical fluxes (such as Rusanov, Godunov or Engquist-Osher) satisfy condition (25). However, there exist monotone numerical fluxes which do not comply with (25), for example $g(a,b) = ((a\top 0)^2 + (b\top 0)^2)/4 - (b^3 - a^3)$ (but it seems to work in practice, which lets us think that condition (25) is purely technical).

Assumption (25) (together with the definition of $g^{\pm}$ via monotone functions $\phi_{l,r}^{\pm}$) makes the last term at the left-hand side of (24) non-positive. Provided the discrete solutions converge, a passage to the limit in (24) as $\Delta t, \Delta x \to 0$ and the consistency of the numerical entropy fluxes $G_{i+1/2}^{\pm}$, $i \neq 0$, yield the Kato inequality:

$$\partial_t |u - v| + \partial_x \Phi(u,v) \leq 0 \quad in\ \mathcal{D}'(\mathbb{R}^+ \times \mathbb{R}), \quad (26)$$

where u, v are the limits of the scheme. The passage-to-the limit argument uses in an essential way the monotonicity of the numerical flux g and the standard device of "weak BV estimates" (see [11]).

Thanks to Prop. 5.1, if $(v_i^n)_{i,n}$ is replaced by $c_L + (c_R - c_L)\mathbf{1}_{\{i>0\}}$ with $(c_L, c_R) \in \mathcal{G}_\alpha^0$ then the limit u of the numerical scheme, if it exists, satisfies (18) with $(c_L, c_R) \in \mathcal{G}_\alpha^0$. In the linear case, thanks to Lem. 5.1, the limit u also satisfies (18) with $(c_L, c_R) \in [0, \lambda] \times [-\lambda, 0]$. Then we use the following lemma:

Lemma 5.2. *(i) Linear drag force: if a function* $u \in L^\infty(\mathbb{R}_+ \times \mathbb{R})$ *verifies the entropy inequalities* (18) *with* $(c_L, c_R) \in \mathcal{G}_l^0 \cup [0, \lambda] \times [-\lambda, 0]$ *then it also verifies* (18) *for all* $(c_L, c_R) \in \mathcal{G}_l$.
(ii) Quadratic drag force: if a function $u \in L^\infty(\mathbb{R}_+ \times \mathbb{R})$ *verifies the entropy inequalities* (18) *for all* $(c_L, c_R) \in \mathcal{G}_q^0$ *then it also verifies* (18) *for all* $(c_L, c_R) \in \mathcal{G}_q$.

In other words, we have justified a Lax-Wendroff kind theorem:

Set

$$u^\Delta(t,x) = \sum_{i \in \mathbb{Z}, n \in \mathbb{N}} u_i^n \mathbf{1}_{[n\Delta t, (n+1)\Delta t[\times [x_{i-1/2}, x_{i+1/2}[}(t,x). \quad (27)$$

If u^Δ is uniformly bounded in $L^\infty(\mathbb{R}_+ \times \mathbb{R})$ and converges a.e. to some limit u, then u is an entropy solution of the Cauchy problem (16), i.e. it satisfies (18) for all $(c_L, c_R) \in \mathcal{G}_\alpha$, $\alpha = l$ or $\alpha = q$ according to the drag force.

It thus remains to obtain *a priori* estimates in order to pass to the limit.

The L^∞-stability of u^Δ is analogous to the statement of Lem. 2.5; it can be proved by classical arguments, using the monotonicity of the scheme. Because of the presence of the singular source term, the numerical scheme is not *TVD*. Moreover, since we are working with a general numerical flux g, a *BV* bound cannot be obtained *via* the use of a Temple function [21]. Therefore, we only prove a BV_{loc} bound, i.e. non uniform in time $BV((-\infty, -\epsilon) \cup (\epsilon, +\infty))$ bound, following the method introduced by Bürger and al. in [9] (see also [10]). The argument of [9] uses the Crandall-Tartar lemma as a starting point; unfortunately, this lemma is designed for conservative methods. Our problem is non-conservative, yet assumption (25) is enough to get the $L^1(\mathbb{R})$ contraction at the discrete level:

$$\Delta x \sum_{i \in \mathbb{Z}} |u_i^{n+1} - v_i^{n+1}| \leq \Delta x \sum_{i \in \mathbb{Z}} |u_i^n - v_i^n| \tag{28}$$

for all discrete solutions $(u_i^n)_{i,n}$, $(v_i^n)_{i,n}$ corresponding to $L^1(\mathbb{R})$ initial data. Indeed, (28) follows readily from Prop. 5.2 and (25), and it can be formally obtained by setting $\varphi(t, x) = \mathbf{1}_{[n\Delta t, (n+1)\Delta t)}(t)$ in Prop. 5.3.

Using (28) and the technique of [9, 10], we deduce the BV_{loc} bound

Lemma 5.3. *Assume that $u_0 \in BV(\mathbb{R})$ and that a classical CFL condition is fulfilled. Let $0 < r < A$ be two real constants and $T > 0$. Then, for Δx sufficiently small, we have*

$$|u^\Delta(T, .)|_{BV([A,+\infty))} \leq |u_0(.)|_{BV([A,+\infty))} + \frac{K}{r}. \tag{29}$$

where K only depends on T, $|u_0|_{BV(\mathbb{R})}$, on the Lipschitz constant of the numerical flux and on the ratio $\Delta t / \Delta x$ (which can be assumed constant).

This lemma is also valid for $A < r < 0$. Note that this estimate blows up as $A \to 0$, but thanks to the L^∞-stability of the numerical scheme, one can extract a converging subsequence by the Cantor diagonal process (see [9] for more details).

We are thus in a position to conclude:

Theorem 5.4. *Assume that $u_0 \in BV(\mathbb{R})$ and D is given by (3) or (4). Then, under a classical CFL condition and condition (25), the numerical scheme (19-22) converges to the unique solution of the Cauchy problem (16)-(13) as $\Delta x \to 0$.*

The extension of the convergence result (and thus, of the existence result) to general $L^\infty(\mathbb{R})$ initial data is a standard issue that can be handled using a regularization of u_0, the principle of finite speed of propagation for the Burgers equation, and the contraction inequalities (28) (discrete) and (15) (continuous).

In the frame of a stationary particle, the numerical scheme (19-22) meets all the requirements we have imposed above since no Riemann solver has been used. Besides, if we are intended to extend this numerical scheme to the case $v_0 \neq 0$, the easiest way is to make the change of variable $\tilde{u}(t, x) = u(t, x - v_0 t)$ and to follow the same construction as before. However, such a trick is equivalent to move the mesh, and it cannot be used if two particles with different velocities are present.

5.2. **The full model.** We present now two numerical methods dedicated to the full model. Both methods are based on a random sampling, for placing the particle at an interface of the mesh at each time step, which avoid the use of a moving mesh. Besides, they do not rely upon a Riemann solver for the full model. The first method is based on the exact Riemann solver for the case of a particle with a constant velocity while the second method is a careful extension of the scheme developed in the previous section.

5.2.1. *A Glimm-like scheme.* This numerical scheme is based on the Glimm scheme and on the exact Riemann solver for (16), that is to say we do not use the Riemann solver for the full model of Sec. 4. Let us describe the main guidelines of this scheme.

1. Start from $(u_i^n)_{i \in \mathbb{Z}}$, h^n and v^n which denote, respectively, the piecewise constant by cell representation of u, the position of the particle (assumed to be at an interface $x_{i+1/2}$ of the mesh) and the velocity of the particle.
2. Solve exactly the Riemann problem for the classical Burgers equation at each interface $x_{i+1/2}$, $\forall i \neq I_n$ where I_n is such that $x_{I_n+1/2} = h^n$.
3. Solve the Riemann problem at the interface $x_{I_n+1/2}$:

$$\begin{cases} \partial_t u + \partial_x (u^2/2) - \lambda D(v^n - u) \, \delta_0(x - v^n t) = 0, \\ u(0, x) = \begin{cases} u_{I_n}^n & \text{if } x < 0, \\ u_{I_n+1}^n & \text{if } x > 0. \end{cases} \end{cases} \tag{30}$$

   Let us recall that the solution of (30) exists, it is unique and it is self-similar (recall that Thm. 3.1 generalizes to the case $v^n \neq 0$). In the following, we denote it by $U(x/t)$.
4. Using a classical CFL condition to prevent any wave interaction between the local Riemann problems, merge all the solutions of the Riemann problems of the two previous steps and obtain a function $\tilde{u}(x)$ composed by constant states separated by discontinuities and affine parts (i.e. rarefaction waves).
5. Compute the trajectory of the particle using an explicit Euler method for the ODE (12):

$$\begin{cases} \tilde{h} = h^n + v^n \Delta t, \\ v^{n+1} = v^n + \dfrac{\Delta t}{m} \big[(U((v^n)^-))^2/2 - v^n U((v^n)^-) \\ \qquad\qquad\qquad - (U((v^n)^+))^2/2 - v^n U((v^n)^+) \big], \end{cases}$$

   where U is the solution of (30). Let us emphasize that the location of the particle in $\tilde{u}$ is exactly $\tilde{h}$. Let us note by $\tilde{I}$ the index of the cell which contains the particle: $\tilde{h} \in [x_{\tilde{I}-1/2}, x_{\tilde{I}+1/2}[$.
6. Take a real $y \in (0, \Delta x)$ by a random (equidistributed) sampling. Define

$$\begin{cases} u_i^{n+1} = \tilde{u}(x_{i+1/2} + y) & \forall i \in \mathbb{Z}, \\ h^{n+1} = \begin{cases} x_{\tilde{I}-1/2} & \text{if } \tilde{h} < y, \\ x_{\tilde{I}+1/2} & \text{if } \tilde{h} > y, \end{cases} \end{cases}$$

Note that, before the random sampling (step 6), this algorithm is conservative with respect to the total impulsion.

5.2.2. *A well-balanced scheme.* This second numerical method takes advantage of two observations. The first one has been mentioned in Sec. 5.2.1 (and it will be illustrated in the next section): the use of the model with a constant velocity at each time step can lead to accurate results. The second observation concerns the fact that the numerical scheme (19-22) is well-suited for the case of a constant velocity, as shown in Sec. 5. Therefore, we are able to construct a numerical scheme for the full model, simply by extension of a monotone flux (see more explanations below) and once more, using a random sampling for the transport of the particle. The method can be described as follows:

1. Start from $(u_i^n)_{i\in\mathbb{Z}}$, h^n and v^n which respectively denote the piecewise constant by cell representation of u, the position of the particle (assumed to be at an interface $x_{i+1/2}$ of the mesh) and the velocity of the particle. Let $I_n \in \mathbb{Z}$ be such that $x_{I_n+1/2} = h^n$.

2. Let g_v be a monotone numerical flux, consistent with the flux $u^2/2 - vu$ (in particular, g_0 is a numerical flux consistent with $u^2/2$). Away from the particle, use a classical scheme:

$$u_i^{n+1} = u_i^n - \frac{\Delta t}{\Delta x}(g_0(u_i^n, u_{i+1}^n) - g_0(u_{i-1}^n, u_i^n)) \quad \forall i \neq I_n, I_n + 1.$$

3. In the two cells near the interface $x_{I_n+1/2}$, use the following well-balanced scheme:

$$(\Delta x + v^n \Delta t)\,\tilde{u}_{I_n}^{n+1} = u_{I_n}^n - \Delta t\,(g_{v^n}(u_{I_n}^n, \phi_\alpha^-(u_{I_n+1}^n)) - g_0(u_{I_n-1}^n, u_{I_n}^n)),$$
$$(\Delta x - v^n \Delta t)\,\tilde{u}_{I_n+1}^{n+1} = u_{I_n+1}^n - \Delta t\,(g_0(u_{I_n}^n, u_{I_n+1}^n) - g_{v^n}(\phi_\alpha^+(u_{I_n}^n), u_{I_n+1}^n)).$$

   Notice that this corresponds to considering two trapezoid cells adjacent to the particle (see Fig.4 and explanations below).

4. Compute the new velocity of the particle:

$$v^{n+1} = v^n - \frac{\Delta t}{m}\big(g_{v^n}(\phi_\alpha^+(u_{I_n}^n), u_{I_n+1}^n) - g_{v^n}(u_{I_n}^n, \phi_\alpha^-(u_{I_n+1}^n))\big).$$

5. Take a real $y \in (0, \Delta x)$ by a random sampling:

$$\text{if } v^n > 0 \begin{cases} u_{I_n}^{n+1} = \tilde{u}_{I_n}^{n+1}. \\ (I_{n+1}, u_{I_n+1}^{n+1}) = \begin{cases} (I_n + 1, \tilde{u}_{I_n}^{n+1}) & \text{if } y < v^n \Delta t, \\ (I_n, \tilde{u}_{I_n+1}^{n+1}) & \text{otherwise,} \end{cases} \end{cases}$$

$$\text{if } v^n < 0 \begin{cases} (I_{n+1}, u_{I_n}^{n+1}) = \begin{cases} (I_n, \tilde{u}_{I_n}^{n+1}) & \text{if } y > -v^n \Delta t, \\ (I_n - 1, \tilde{u}_{I_n+1}^{n+1}) & \text{otherwise,} \end{cases} \\ u_{I_n+1}^{n+1} = \tilde{u}_{I_n+1}^{n+1}. \end{cases}$$

Let us explain this algorithm with the help of Fig. 4. First, the trajectory of the particle is computed using the explicit Euler method and thus, the trajectory is piecewise affine. After, the model is integrated of the trapezoids

$$\{(x, t) \text{ such that } x \in (x_{I_n-1/2}, x_{I_n+1/2} + v^n(t - t^n)), t \in (t^n, t^{n+1})\},$$

$$\{(x, t) \text{ such that } x \in (x_{I_n+1/2} + v^n(t - t^n), x_{I_n+3/2}), t \in (t^n, t^{n+1})\}$$

(see Fig. 4, the trapezoids are dashed). Eq. (1) in these trapezoids reduces to the homogeneous Burgers equation but, since the interface due to the particle is inclined, the numerical flux through it must be consistent with $u^2/2 - v^n u$. These integrations over the trapezoids lead to the formulae of step 3 and allow to define $\tilde{u}_{I_n}^{n+1}$ and $\tilde{u}_{I_n+1}^{n+1}$, the first one corresponding to the interval $(x_{I_n-1/2}, x_{I_n+1/2}+v^n\Delta t)$
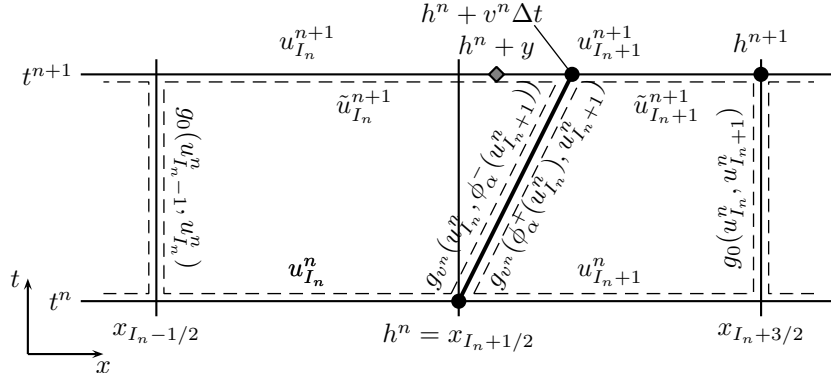
FIGURE 4. Representation of the algorithm based on the well-balanced scheme.

and the second one to the interval $(x_{I_n+1/2} + v^n \Delta t, x_{I_n+3/2})$. The update is done by random sampling. In Fig. 4, the random variable satisfies $0 < y < v^n \Delta t$, which means that the point $h^n + y$ belongs to the interval of $\tilde{u}_{I_n}^{n+1}$, providing $u_{I_n}^{n+1} = \tilde{u}_{I_n}^{n+1}$, $u_{I_n+1}^{n+1} = \tilde{u}_{I_n}^{n+1}$ and $I_{n+1} = I_n + 1$. Finally, the velocity of the particle is updated; the formula of Step 4 is obtained by the conservation of the total momentum (before the random sampling of Step 5, which breaks the conservation of momentum).

5.2.3. *Numerical results.* The first test case is a Riemann problem, over the domain $[0, 1]$. The initial data are for the fluid $(u_L, u_R) = (0, -2)$ and for the particle $(h(0), h'(0)) = (0.5, 15)$. The drag force is linear with $\lambda = 10$ and the mass of the particle is $m = 0.1$. This test case corresponds to to case (III) in [18].

For small times, the solution is composed by a rarefaction wave moving to the right, which connects u_L to $u_* = u_R + \lambda$, and by the discontinuity separating u_* and u_R (this discontinuity is due to the particle which is located at the discontinuity). After a while, the intermediate state u_* disappears, when the rarefaction wave catches up the particle. At the end, the rarefaction wave also vanishes and the solution is only composed by a discontinuity between u_L and u_R and the particle is overlaid on this discontinuity. The velocity of the particle (and, as a result, of the discontinuity) tends to $(u_L + u_R)/2$ as $t \to +\infty$ (see [18] for explicit formulae).

In Fig. 5 are plotted several results obtained by the Glimm-like scheme for successive times, over 1000 cells, with a Courant number equal to 0.4. One can note that the qualitative behavior of case (III) in [18] is very well reproduced.

In Fig. 6 are compared the results obtained by both numerical methods (WB: well-balanced scheme, Gl: Glimm scheme) over 1000 cells, with a Courant number equal to 0.4, at $t = 0.2$ (the solution composed by a rarefaction wave, from $x = 0$ to the position of the particle). The numerical flux used for the well-balanced scheme is the Godunov scheme. One can see in Fig. 6 that the discontinuity due to the particle are perfectly resolved by the numerical methods. However, since both methods depend on a sequence of random variables (we actually use the low-discrepancy van der Corput sequence, *randomly initialized*), it is not relevant to compare the results given by each method. Indeed, the fact that the position of the particle is the same with both schemes is a coincidence.
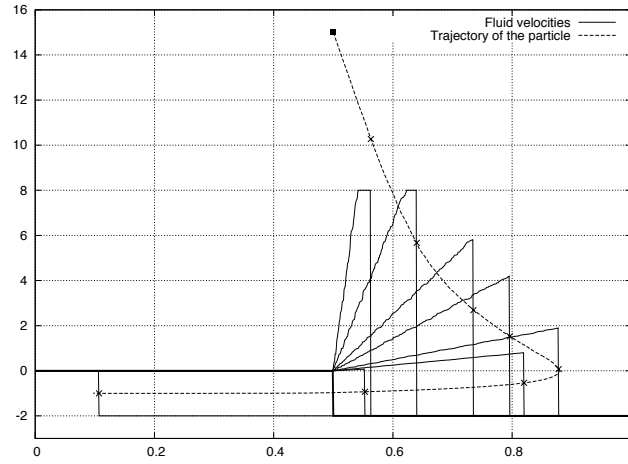
FIGURE 5. Velocities of the fluid and of the particle w.r.t. x computed by the Glimm scheme, at times 0, 0.5×10^{-2}, 1.5×10^{-2}, 4×10^{-2}, 7×10^{-2}, 0.2, 0.4, 0.75 and 1.2.
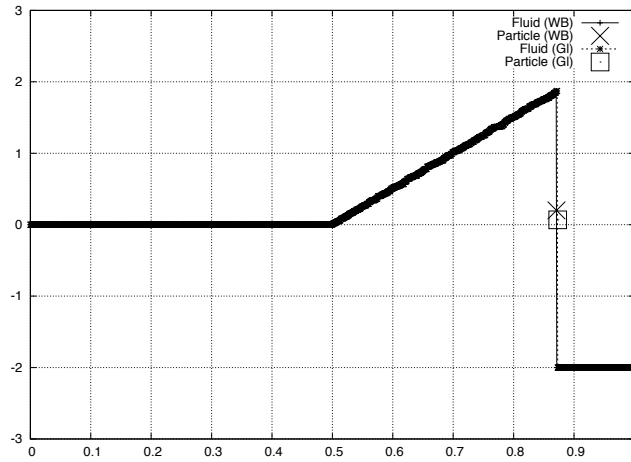

FIGURE 6. Comparison of the two methods (velocity of the fluid and of the particle w.r.t. x)

In order to provide a more appropriate comparison, we provide the result of 1000 simulations and present in Fig. 7 the associated probability density functions of the velocity of particles. The random sampling used in each method follows a uniform distribution and the resulting probability density functions for the velocity in Fig. 7 seem to follow a normal distribution. They are very close (i.e. less than 5 %): the difference between the expected values of velocity is about 0.003, while the expected velocity is about 0.066.

We now present a numerical test with two particles, in the case of a linear drag force (3), assuming that no collision can occur but only perfect crossings. We have used the first numerical scheme and a classical splitting method for the extension
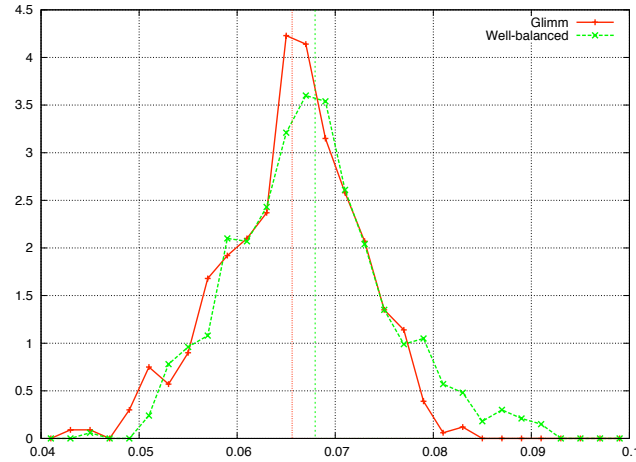
FIGURE 7. Probability density function of the velocity of the particle computed by each method

to two particles. The corresponding model writes, for $t \in [0, 5]$ and, as $x \in [0, 1]$

$$\begin{cases} \partial_t u + \partial_x u^2/2 = (h_1'(t) - u) \, \delta_0(x - h_1(t)) + (h_2'(t) - u) \, \delta_0(x - h_2(t)), \\ m_1 h_1''(t) = u(t, h_1(t)) - h_1'(t), \qquad m_2 h_2''(t) = u(t, h_2(t)) - h_2'(t), \\ u(0, \cdot) = 0, \qquad (h_1(0), h_1'(0)) = (0.2, 1), \qquad (h_2(0), h_2'(0)) = (0.3, 1), \end{cases}$$

where $m_2 = 2 \times 10^{-2}$ (note that $\lambda = 1$ and that the drag force is linear). The boundary conditions are periodic but they actually are inactive. We present in Fig. 8 the trajectories of the particles for $m_1 = 1.5 \times 10^{-2}$, 2×10^{-2} and 2.5×10^{-2}, computed using 10000 cells and a Courant number of 0.3. We can see in each case the so-called *drafting-kissing-tumbling* phenomenon. At the beginning, both particles are slowed down by the fluid, but once particle 1 is in the wake of particle 2, its velocity becomes about constant, while the velocity of particle 2 continue to decrease. After a while, the particles cross: particle 1 is ahead. After the crossing, particle 2 is in the wake of particle 1, which is slowed down by the fluid, and thus accelerate. And a new crossing occurs... See Fig. 8(bottom) which includes a zoom near the first crossings. The numerical scheme provides very accurate results, in the sense that the *drafting-kissing-tumbling* is well reproduced.

6. **Conclusion.** We have presented several theoretical and numerical results about a simple model of interaction between an inviscid fluid, modeled by the Burgers equation, and a point-wise particle, *via* a drag force. Despite its simplicity, it can reproduce complex phenomena and seems a good starting point to more complex models, including for instance the interaction of point-wise particles with a fluid modeled by the compressible Euler equations (some encouraging progresses have already been done in this direction). Concerning the analysis, several questions remain, in particular about the well-posedness (uniqueness, continuous dependence on the data) of the Cauchy problem for the full model (1-2) and about the convergence of the numerical method presented in the last section.
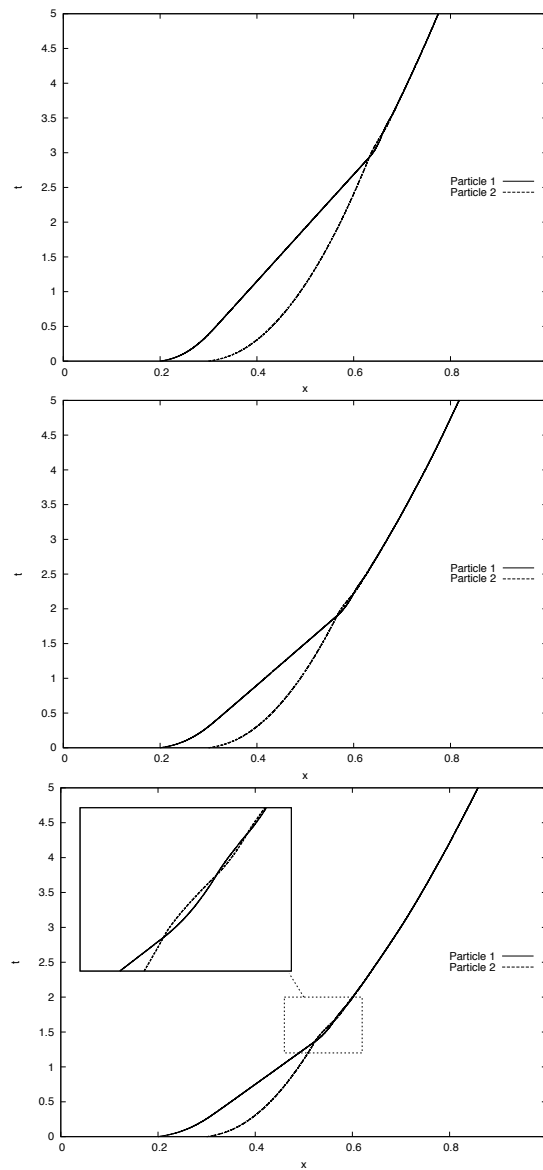
FIGURE 8. Trajectories of the particles for $m_1 = 1.5 \times 10^{-2}$ (top), $m_1 = 2 \times 10^{-2}$ (middle) and $m_1 = 2.5 \times 10^{-2}$ (bottom).

article started as part of the international research program on Nonlinear Partial Differential Equations at the Centre for Advanced Study at the Norwegian Academy of Science and Letters in Oslo during the academic year 2008–09.

REFERENCES

[1] B. Andreianov, K. H. Karlsen and N. H. Risebro, *A theory of L^1-dissipative solvers for scalar conservation laws with discontinuous flux*, Preprint, appeared on the Conservation Laws Preprint Server (http://www.math.ntnu.no/conservation/).

[2] B. Andreianov, K. H. Karlsen and N. H. Risebro, *On vanishing viscosity approximation of conservation laws with discontinuous flux,* Preprint, appeared on the Conservation Laws Preprint Server (<http://www.math.ntnu.no/conservation/>).

[3] B. Andreianov and N. Seguin, *Well-posedness of a singular balance law,* In preparation.

[4] B. Andreianov, F. Lagoutière, N. Seguin and T. Takahashi, In preparation.

[5] Adimurthi, S. Mishra and G. D. Veerappa Gowda, *Optimal entropy solutions for conservation laws with discontinuous flux-functions,* J. Hyperbolic Diff. Eq., **2** (2005), 783–837.

[6] E. Audusse and B. Perthame, *Uniqueness for scalar conservation laws with discontinuous flux via adapted entropies,* Proc. Roy. Soc. Edinburgh Sect. A, **135** (2005), 253–265.

[7] F. Bachmann and J. Vovelle, *Existence and uniqueness of entropy solution of scalar conservation laws with a flux function involving discontinuous coefficients,* Comm. Partial Differential Equations, **31** (2006), 371–395.

[8] P. Baiti and H. K. Jenssen, *Well-posedness for a class of 2×2 conservation laws with L^∞ data,* J. Differential Equations, **140** (1997), 161–185.

[9] R. Bürger, A. García, K. H. Karlsen and J. D. Towers, *A family of numerical schemes for kinematic flows with discontinuous flux,* J. Engrg. Math., **60** (2008), 387–425.

[10] R. Bürger, K. H. Karlsen and J. D. Towers, *An Engquist–Osher-type scheme for conservation laws with discontinuous flux adapted to flux connections,* SIAM J. Numer. Anal., **47** (2009), 1684–1712.

[11] R. Eymard, T. Gallouët and R. Herbin, "Finite Volume Methods," In "Handbook of Numerical Analysis, Vol. VII," Handb. Numer. Anal., VII, pages 713–1020. North-Holland, Amsterdam, 2000.

[12] L. Gosse and A.-Y. LeRoux, *Un schéma-équilibre adapté aux lois de conservation scalaires non-homogènes,* C. R. Acad. Sci. Paris Sér. I Math., **323** (1996), 543–546.

[13] J. M. Greenberg and A.-Y. LeRoux, *A well-balanced scheme for the numerical processing of source terms in hyperbolic equations,* SIAM J. Numer. Anal., **33** (1996), 1–16.

[14] M. Hillairet, *Do Navier-Stokes equations enable to predict contact between immersed solid particles?* In "Analysis and Simulation of Fluid Dynamics," Adv. Math. Fluid Mech., pages 109–127. Birkhäuser, Basel, 2007.

[15] E. Isaacson and B. Temple, *Convergence of the 2×2 Godunov method for a general resonant nonlinear balance law,* SIAM J. Appl. Math., **55** (1995), 625–640.

[16] K. H. Karlsen, N. H. Risebro and J. D. Towers, L^1 *stability for entropy solutions of nonlinear degenerate parabolic convection-diffusion equations with discontinuous coefficients,* Skr. K. Nor. Vidensk. Selsk., **3** (2003), 1–49.

[17] K. H. Karlsen and J. D. Towers, *Convergence of the Lax-Friedrichs scheme and stability for conservation laws with a discontinous space-time dependent flux,* Chinese Ann. Math. Ser. B, **25** (2004), 287–318.

[18] F. Lagoutière, N. Seguin and T. Takahashi, *A simple 1D model of inviscid fluid-solid interaction,* J. Differential Equations, **245** (2008), 3503–3544.

[19] E. Yu. Panov, *Existence of strong traces for quasi-solutions of multidimensional conservation laws,* J. Hyperbolic Differ. Equ., **4** (2007), 729–770.

[20] N. Seguin and J. Vovelle, *Analysis and approximation of a scalar conservation law with a flux function with discontinuous coefficients,* Math. Models Methods Appl. Sci., **13** (2003), 221–257.

[21] B. Temple, *Global solution of the Cauchy problem for a class of 2×2 nonstrictly hyperbolic conservation laws,* Adv. in Appl. Math., **3** (1982), 335–375.

[22] J. D. Towers, *Convergence of a difference scheme for conservation laws with a discontinuous flux,* SIAM J. Numer. Anal., **38** (2000), 681–698.

E-mail address: `boris.andreianov@univ-fcomte.fr`
E-mail address: `frederic.lagoutiere@math.u-psud.fr`
E-mail address: `seguin@ann.jussieu.fr`
E-mail address: `takeo.takahashi@iecn.u-nancy.fr`